Scots pines colonizing the harsh environment of volcano slopes increased their hydraulic safety margin

Têtè Sévérien Barigah, Fernanda dos Santos Farnese, Paulo de Menezes Silva, Paul Humbert, Mustapha Ennajeh, Jérôme Ngao, Eric Badel, Hervé Cochard, Stéphane Herbette

Scots pines colonizing the harsh environment of volcano slopes increased their hydraulic safety margin

Têtè Sévérien Barigah[1], Fernanda Dos Santos Farnese[2], Paulo De Menezes Silva[2], Paul Humbert[1], Mustapha Ennajeh[3], Jérôme Ngao[1,†], Eric Badel[1], Hervé Cochard[1], Stephane Herbette[1]

[1]Université Clermont Auvergne, INRAE, PIAF, 63000 Clermont-Ferrand, France

[2] Laboratory of Plant Stress Physiology, Instituto Federal de Educação, Ciência e Tecnologia Goiano, Campus Rio Verde, 75906- 820 Rio Verde, GO, Brazil

[3] Laboratory of Biodiversity and Valorization of Bioresources in Arid Zones, Faculty of Sciences of Gabes-City Erriadh, Zrig, Gabes 6072, Tunisia

Full address of the corresponding author
Stéphane Herbette
UMR INRAE/UCA 547 PIAF
Université Clermont Auvergne, Campus Universitaire des Cézeaux,
1 Impasse Amélie Murat,
TSA 60026, 63178 AUBIERE Cedex
FRANCE
Stephane.Herbette@uca.fr

† Present address: Institut Agro, Eco&Sols, Université Montpellier, CIRAD, INRAE, IRD, 34060 Montpellier, France

Acknowledgements

We are grateful to the AgroClim unit for providing meteorological data, to Pierre Conchon and Marc Vandame for field and lab assistance.

Abstract

The ability of trees to survive and naturally regenerate under increasing drought conditions will depend on their capacity to vary key hydraulic and morphological traits that increase drought tolerance. Yet, there has been limited investigation into this variability under recurrent severe drought conditions since the establishment phase. We investigated the hydraulic and leaf trait adjustments of Scots pine trees settled in an abandoned slag quarry by comparing them across three topographic positions inducing contrasted effects on growth. We measured xylem and foliar traits to compare the water status of trees according to tree location and to evaluate the respective risk for xylem hydraulic failure using the soil-plant hydraulic model *SurEau*. Compared to upslope and downslope trees, slope trees exhibited lower growth, photosynthetic pigment contents, vulnerability to embolism and specific hydraulic conductivity as well as higher water potential at turgor loss point and midday water potentials. As a consequence, slope trees showed an increase in the hydraulic safety margin and a low level of embolism, compared to downslope and to upslope trees.. Additionally, these adjustments induced an increase in the time to hydraulic failure in slope trees compared to downslope and upslope trees under similar drought conditions simulated using the *SurEau* model. These results suggest a prioritization of hydraulic safety over growth in Scots pine developed in a harsh environment, resulting in a dwarf phenotype.

Key words: Acclimation, embolism, mortality, *Pinus sylvestris* L., pioneer species, water stress

Key message: Scots pines developed for several years on volcano slopes showed a dwarf phenotype and a larger hydraulic safety margin than downslope trees, such that hydraulic safety was prioritized over growth.

Introduction

Tree species with a wide distribution area or living in contrasting habitats, and pioneer species, must display variability for traits that allow them to cope with various environmental conditions. Especially, the soil water availability is critical in seedling establishment, plant growth and survival. Successful seedling and sapling development is a prerequisite for forest regeneration as well as for pioneer colonization (Lloret et al. 2009). Impeding these stages under climate change would hamper forest establishment and regeneration (Anderson-Teixeira et al. 2013).

A wide range of structural and physiological adjustments based on phenotypic plasticity and genetic variability is a key feature for tree species adaptation to environmental changes, especially for pioneer species (Sultan et al. 2000; Nicotra et al. 2010). Indeed, species with greater plasticity may be more likely to survive climate change that occurs too rapidly to allow for a population migration or an evolutionary response. Moreover, plasticity allows pioneer species to colonize environmentally diverse sites without the lag time required for local adaptation. Studying variations of traits related to drought resistance is necessary to improve the predictions of tree responses to climate change (Anderegg 2015).

Resistance to drought is conferred by a set of interacting traits, in which hydraulic traits have a key role (Martínez-Vilalta et al. 2002; Chaves et al. 2003; Choat et al. 2012). Indeed, drought-induced tree mortality is mainly due to xylem hydraulic failure caused by embolism (Barigah et al. 2013; Anderegg et al. 2016), even if functional evidence remains to be found to link hydraulic failure and tree death (Mantova et al. 2022). Much is known about the variability of these hydraulic traits across species (Maherali et al. 2004; Jacobsen et al. 2007; Choat et al. 2012), and about their intraspecific variability (e.g. in Martinez-Vilalta et al. 2009; Herbette et al. 2010; Bartlett et al. 2014; González-Muñoz et al. 2018). Within species variations in hydraulic traits have been reported for many species grown under natural conditions (Martínez-

Vilalta et al. 2009; González-Muñoz et al. 2018), in common gardens (Wortemann et al. 2011; Lamy et al. 2011; Pritzkow et al. 2020) or under controlled experimental conditions (Awad et al. 2010; Lemaire et al. 2021). Yet, little is known about the physiological adjustment capacities of pioneer trees establishing in bare sites under severe water deficit conditions. Studies comparing hydraulic properties along wide environmental gradients for a given species provide information on the extent of trait variations in mature trees and within the species' range, but this did not consider the tree settlement phase for pioneer species and did not reflect the effects of predicted more severe droughts than those undergone in their present niche. Conversely, most studies based on drought manipulation experiments submitted trees to severe drought but they were typically short-term or did not consider the tree settlement phase (Cotrufo et al. 2011; MacKay et al. 2012; Herbette et al. 2021; Moreno et al. 2021). Yet, acclimation processes and long-term mechanisms could occur to adjust tree responses to changes in water availability on longer time scales (Leuzinger et al. 2011; Barbeta et al. 2013; Feichtinger et al. 2014). For a full understanding of the drought resistance strategy of pioneer species, the leaf traits need also to be considered, as they reflect the tree strategy regarding the water losses as well as the use of other resources (Wright et al. 2004; Bartlett et al. 2012). Moreover, trees can adjust their water consumption and hydraulic safety through the coordination of stomatal regulation and modification of the hydraulic system (Choat et al. 2012; Martínez-Vilalta et al. 2009; Rosas et al. 2019). The leaf water potential at turgor loss (Ψ_{tlp}) and its related parameters have been proposed as powerful indicators of the drought tolerance of plants (McDowell 2011; Bartlett et al. 2012). Indeed, plants with lower Ψ_{tlp} are more efficient to maintain stomatal conductance, photosynthesis, hydraulic conductance, and growth under water stress (Bartlett et al. 2012). Despite stomatal closure, water loss continues through the cuticle and incompletely closed stomata, and this is measured as the leaf minimum conductance (g_{min}). Recent studies showed this trait to be critical, especially for severe droughts (Duursma et al. 2019; Brodribb et al. 2020).

Under long-term drought conditions, tight coordination between hydraulic and leaf traits should allow plants to balance between safety (avoiding hydraulic failure) and efficiency, in terms of resource use to ensure growth and maintenance (Brodribb et al. 2014). Therefore, to better understand pioneer settlement in harsh habitats and to predict forest development under climate change, investigations are needed on the impact of drought on hydraulic and leaf traits over a longer period starting from seedling establishment.

Scots pine (*Pinus sylvestris* L.) spans a vast climatic gradient from Eastern Siberia to Southern Spain (Poyatos et al. 2007). It is a pioneer tree establishing on wet or dry sites, on poor, sandy soils, rocky outcrops, peat bogs and other various harsh ecosystems (Richardson and Rundel 1998). Although this species is considered to be drought resistant, more than one-third of the drought-induced forest diebacks reported by Allen et al. (2010) are linked to Scots pine forests. These features make this species relevant for the study of the variability in drought-resistant traits, in addition to economic reasons and its importance in successional dynamics of temperate forests and thus their sustainability. That is why trait variability has been studied in Scots pine, especially for hydraulic traits (Poyatos et al. 2007; Martinez-Vilalta et al. 2009; Zang et al. 2012; Feichtinger et al. 2015; Seidel and Menzel 2016; Rosas et al. 2019), and for other traits related to cambial activity (Fernández-de-Uña et al. 2018) or leaf area/sapwood area ratio (Mencuchini and Bonosi 2001). However, more comprehensive investigations on hydraulic traits variability and their interactions during the settlement phase are also needed under extremely dry conditions to complete the picture of physiological and structural hydraulic plasticity in this pioneer species. This will contribute to improve our understanding of the colonization mechanisms of pioneer trees and help predict how climate change will affect this species.

We identified an abandoned quarry that had been exclusively colonized by Scots pines for 20 years, with no other vegetation able to settle, allowing to investigate adjustments mechanisms

(throughout selection and/or acclimation) over many years under very constraining environmental conditions (Figure 1). The trees established at slope position displayed greatly reduced dimensions of plants, annual shoots and needles and yellowing of needles when compared to individuals established downslope or upslope. In this study, we compared water relations of trees located in these different positions and we evaluated morphological and hydraulic traits at needle and stem levels that allowed this species to establish within such a harsh environment. We hypothesized that 1) Scots pine shows large difference between topographic conditions for both leaf and stem hydraulic traits including vulnerability to embolism, hydraulic conductivity, turgor loss point 2) the subsequent hydraulic adjustments in slope trees allow Scots pine trees to operate with a narrow hydraulic safety margin and at higher risk of mortality, 3) the slope trees display a higher native embolism level and a lower growth than at the other positions due to hydraulic limitations.

Materials and methods

Site and trees

The site was located aside the East hillside of the volcano "Puy de la Vache", (Saint-Genès-Champanelle, France), at an altitude of 962 to 973 m (45°42′ N, 2°58′ E), in a scoria quarry abandoned in the 1980's. The soil substratum is scoria, a dark colored basaltic or andesitic volcanic rock. The site was characterized by loose substratum, low field capacity, nutrient poverty, high solar irradiation and temperature, recurrent summer droughts and cold winters (Frain 1991). It was a former reserve of scoria and the company that operated the quarry shaped the landscape (Figure 1) removing soil, exposing slag substrate and shaping the relief over a short distance into terraces, foothills and hillslopes.

On the site, Scots pines developed in a large open patch free of plant as the ground was left bare (Figure 1). We divided the studied trees in three groups regarding their location in the landscape and their statures. The slope trees were shrubby and small with reduced needle size,

while the downslope trees were vigorous and tall with larger needles and the upslope ones were intermediate (figure 1). We selected trees far from the border between two positions. Moreover, we also checked that the selected trees showed the morphological differences that distinguish the three groups, especially between slope and downslope trees. We selected trees of homogeneous ages, from 17 to 23 years old, and an average of 18.8 years' old over all groups. Most measurements were carried out during the spring and summer of 2013. Some additional measurement such as the chlorophyll, carotenoids and mineral contents were performed during the summer 2018.

Branch age and growth

The age of the sampled branches was assessed by the number of wood rings.

Annual ring growth was measured on the branches collected for measurements of hydraulic traits and needle parameters. Mean annual ring growth was calculated as the total wood diameter over the number of rings for 31, 39 and 25 branches from downslope, upslope and slope trees, respectively.

Needle chemical nutrient, chlorophyll and carotenoid content assays

We determined the contents of nitrogen (N), calcium (Ca), potassium (K), magnesium (Mg), sodium (Na), iron (Fe), copper (Cu), zinc (Zn) and plumb (Pb) on newly-developed needles sampled from three to five trees per location. The needles were taken from branches at the top of the trees and exposed to sunlight. Needles were dried in a forced-air oven for 48 h at 80°C. Then, we determined the total N content using the Kjeldahl method (Kjeldahl 1883), while we quantified Ca, K, Mg, Na, Fe, Cu, Zn and Pb by atomic spectrometric absorption method, as described in Paula et al. (2014). First, we mineralized the samples of 20 mg of dried needle material in 35% nitric acid and evaporated to dryness on a hotplate. We then dissolved the minerals in 0.1 N HCl solution. Afterward, we filtrated the solution on Whatman paper N°1. Finally, we measured the ion concentrations with an atomic absorption spectrometer (Avanta

GBC spectrometer, Australia), using an air-acetylene flame. We reproduced this process thrice to evaluate a mean value for each sampled tree.

To assay the chlorophyll (Chl) and carotenoid contents of the needles, we relied on a procedure adapted from Minocha et al. (2009) and sampled newly developed needles from 8 to 15 individual trees for each location and put them immediately in a cooler that contained crushed ice and brought them back to the laboratory. We transferred the samples in liquid nitrogen and stored them at -80 °C until analysis.

Needle xylem water potentials

Six to eight trees per location were used for measurements of needle midday needle water potential (Ψ_{md}) during the season of 2013, and five trees for daily time course of needle water potentials (Ψ_{needle}) on August 21st, 2013. We completed the Ψ_{md} measurements between 11.00 am and 1.00 pm solar time. We processed the shoots on the field with a Scholander-type pressure chamber (PMS, Corvallis, Oregon, USA) on covered small shoot tips sampled from sunlight exposed south-facing shoots.

Foliar traits

The specific needle area (SLA) was calculated as the needle area divided by its dry weight. The needle area was evaluated using the length and diameters and considering the needle shape as an ellipse. We measured the SLA on 10 newly-developed needles per tree and on five trees from each location.

The Huber value (H_v) is the ratio of cross-sectional sapwood area to subtended leaf area, and it can therefore be analyzed as the ratio of hydraulic and mechanical investment costs over the expected gains obtained by leaf display. The whole needles from terminal branches were oven-dried and weighed, and SLA was used to convert the total dry weight of the distal needles of each branch into total branch needle area. Sapwood area was estimated by measuring the

total xylem area on digital images of scanned cross-sections of the collected branches using ImageJ software (Wayne Rasband-National Institute of Health).

The needle-cell turgor features were computed using pressure-volume curves (p-v curves). The bench dehydration method was used (Tyree and Hammel 1972; Sack and Pasquet-Kok 2010). We cut 50 cm long shoot samples located at the top of trees and exposed to sunlight from eleven to thirteen trees per location and immediately placed them in plastic bags with wet paper towels to bring them in the laboratory. The samples were rehydrated at full turgor by putting the cut end in water at room temperature overnight in a sealed bag and in a dark room. Then, shoots bearing needles were allowed to dehydrate while periodically being weighed and measured for water potential (Ψ) using a pressure chamber (1505D, PMS Instrument). To prevent rapid water loss, the shoot samples could be kept in plastic bags between measurements. When Ψ was lower than -4 MPa, we measured the needle area, and the entire shoots were dehydrated in an oven at 70 °C during 72 h to reach the needle dry weight. The p-v curve was plotted using the inverse values of needle water potential versus the relative water content (RWC) which was obtained from repeated determinations of fresh mass during dehydration of the shoot tips. Several parameters can be extracted from the p–v curves (Tyree and Hammel 1972; Sack and Pasquet-Kok 2010) : the osmotic potential at full turgor (π_0) and the water potential at turgor loss point (Ψ_{TLP}), the water content at full turgor (WC_0) calculated as the mass of water per needle dry mass, the relative water content at turgor loss point (RWC_{TLP}) and the bulk modulus of tissue elasticity (ε_0).

The minimal needle conductance (g_{min}) was also determined using data from p-v curves (detailed above). The g_{min} was determined from the slope of the linear part of the curve after stomatal closure, and adjusted for needle area of the sample and for temperature and humidity regularly scored during measurements.

Hydraulic traits

To visualize xylem embolism, we relied on X-ray microtomograph observations, which is a reference method (Cochard et al. 2015). We excised 0.3m-long xylem segments from branches located at the top of the trees and exposed to sunlight from two trees per location, wrapped them in humid paper and plastic bag, brought to the laboratory for analyses on the same day. We removed the needles under water and sealed them in liquid paraffin wax in order to prevent dehydration during the X-ray scans. We placed the samples in an X-ray microtomograph (Nanotom 180 XS, GE, Wunstorf, Germany). The field of view was 5 × 5 × 5 mm and covered the full cross section of the samples. The X-ray source settings were 50 kV and 275 μA. For every 40-min scan, we recorded 1000 images during the 360° rotation of the sample. After 3D reconstruction, the spatial resolution of the image was 2.5 × 2.5 × 2.5 μm per voxel. We extracted the transverse 2D slice from the middle of the volume and used ImageJ software for visualization and image analysis.

Vulnerability to embolism was measured on branches located at the top of the trees and exposed to sunlight. Branches of 0.4–0.5 m long were harvested from at least five individuals per location, wrapped in humid paper and plastic bag, brought to the laboratory and stored at 4°C until measurements in the following days, up to one week after sampling. We cut stem segments of 0.28 m-long just before the measurement of their vulnerability to cavitation with the Cavitron technique (Cochard et al. 2005). We measured the loss of hydraulic conductance of the stem segment while the centrifugal force generated an increasing negative xylem pressure. The plot of the percent loss of xylem conductance (PLC) versus the xylem pressure represents the vulnerability curve. First, we set the xylem pressure to a reference pressure (-0.5 or –1.0 MPa) and we determined the maximal conductance (k_{max}) of the sample. Then, we set the xylem pressure to a more negative pressure for 2 min, and we determined the new conductance (k). The procedure was repeated for more negative pressures (with –0.50 MPa increments) until

PLC reached at least 90%. We generated vulnerability curves for each branch by fitting the data with exponential–sigmoidal function (Pammenter and Willigen 1998):

$$PLC = \left[\frac{100}{1 + e^{\{s / 25(P - P_{50})\}}} \right] \quad (6)$$

Where P_{50} is the pressure causing 50% loss of conductance and s is the slope value at this point.

Specific hydraulic conductivity (K_s) was measured on branches collected from the top of trees and exposed to sunlight from six individual trees per location. The day after sampling, branch segments were recut underwater using a razor blade and their length (L_{stem}) was measured. The apical end of the sample was plugged to an embolism meter (Xyl'em, Bronkhorst, Montigny les Cormeilles, France). The total conductance (K) was then measured under low pressure (2–7 kPa) using a solution of 10 mM KCl and 1 mM $CaCl_2$. The xylem area A_x was measured as the mean area of the both ends of the sample on digital images of scanned cross-sections in ImageJ. The K_s was defined as follows:

$$K_s = K \times L_{stem} / A_x. \quad (7)$$

Leaf specific conductivity (LSC) was measured on the same samples and was determined by replacing Ax to the subtended leaf area. This leaf area was measured as previously described.

SurEau model simulations

The *SurEau* model is a mechanistic discrete-time soil–plant–atmosphere hydraulic model that predicts plant hydraulic and hydric properties under simulations of water stress (Martin St Paul et al. 2017; Cochard et al. 2021). It is used to simulate the time to hydraulic failure under drought considering that this time is reached with high embolism level, i.e. 90 % (e.g. Lemaire et al. 2021). In this work, we used the *SurEau* model to understand how the combination of tree traits measured in the 3 quarry ecological conditions impacted their time to

reach hydraulic failure. We parameterized the trees of each condition in the model by taking into account their average size, estimated in the field, and the physiological parameters that we measured (see Table S1 available as Supplementary Data at *Trees* Online for an exhaustive list of variables). For the soil, we considered that the surface explored by the roots was the same as the surface of the crowns and that the ratio between the volume of water available in the soil and the leaf surface was constant. This defined the soil depth in each condition. The hydric and hydraulic properties of the soil were described by pedotransfer functions according to the model of van Genuchten (1980) adapted to scoria (Wallach et al 1992). We considered stomatal conductance to be a linear function of needle turgor pressure calculated from the pressure-volume curve parameters. The water potential at stomatal closure was assumed to coincide with the turgor loss point. The bark conductance was assumed to be equal to the minimum conductance measured on leaves. The exhaustive list of variables can be found in the table S1 at *Trees* Online. The model was run under constant climate conditions set to match the climate conditions in the field at noon on a typical sunny day in June, with the atmospheric temperature set at 28 °C, the atmospheric relative humidity set at 25% and the PAR set at 1000 μmol m^{-2} s^{-1}. The wind speed was set at 1 m s^{-1}. In a first case, simulations are made for each type of tree in their respective environments. The combined effects of morphological and physiological parameters on hydraulic failure are then taken into account. In the next two cases, we simulated trees in a downslope and slope position but applied the physiological traits measured under the other site conditions. Here, the morphological differences between the conditions are ignored. The results of the simulations are given in terms of the temporal dynamics of PLC of the branches.

Statistical analysis

We subjected measured and derived data to statistical analysis using a software package (XLSTAT 19.4.46926, Addinsoft, Paris, France) for ANOVA. We compared the mean values with Tukey's multiple range tests at 0.05 levels when effects were significant.

Results

To measure foliar and hydraulic traits, we had to collect branch samples of homogeneous dimensions. The samples showed therefore differences in age, especially between downslope and upslope trees (figure 2). The slope trees showed a significantly lower annual ring growth rate over years ($P<0.001$) compared to downslope and the upslope trees. To test if slope, even upslope, trees suffered from nutrient deficiency, we measured the main chemical elements of the needles (table 1). Except for nitrogen, there was no difference in needle nutrient contents between the locations. Both upslope and slope trees displayed similar nitrogen content (8.54 ± 0.35 and 7.16 ± 0.49 mg g^{-1} DW), contrary to the downslope trees that had higher content of nitrogen (12.85 ± 1.03 mg g^{-1} DW). The total needle chlorophyll and carotenoid contents were also variable regarding the tree locations (table 2), They were significantly higher in the downslope trees compared to the slope and upslope trees. To compare the water status of trees according to their position, we monitored the evolution of needle midday water potential (Ψ_{md}) over the growing season (figure 3A). At the onset of the experiment, we found no significant difference in Ψ_{md} between locations. Then, the Ψ_{md} decreased over the season but stabilized earlier for the slope trees than for the upslope and downslope ones. Consequently, the slope trees had a significantly higher Ψ_{md} (about – 1.0 MPa) compared to the upslope and downslope ones (up to -1.5 MPa). The Ψ_{md} were similar for both upslope and downslope trees (figure 3A). On day 233, sunniest and driest day in late summer of the year, we carried out a survey of needle water potentials (Ψ, figure 3B). At predawn (i.e. before 7 am), no significant difference in Ψ was found between trees from the three locations. Then, the Ψ decreased over time but stabilized earlier for the slope trees than for the upslope

and downslope ones. Consequently, the slope trees had a significantly higher Ψ compared to the upslope and downslope ones, during this day (figure 3B). We found similar results for day 214, which was another almost cloudless and very dry day in the same summertime (data not shown).

To investigate the drought resistance strategy according to the trees' location, we measured hydraulic and foliar traits. We measured the xylem vulnerability to embolism on branches (figure 4 A). The slope trees were more resistant to embolism than downslope trees with branch P_{50} values of -3.70 MPa and -3.25 MPa, respectively, while the upslope trees displayed an intermediate P_{50} value of -3.49 MPa (table 3). The X-ray microtomography observation revealed that the native embolism in the tested trees was rather low (less than 5 %) regardless their location, and no embolism did occur over the last years (figure 5). This excludes possible effect of native embolism on the measured P_{50}. The branches from slope trees showed also a significantly lower mean value for K_s and *LSC* compared to upslope and downslope trees (table 3).

At the needle level, the SLA showed significant differences according to the tree location, the SLA being significantly higher in slope trees compared to downslope and upslope trees. The bulk leaf parameters drawn from the p-v curves revealed a lower Ψ_{TLP} for slope trees compared to downslope trees (table 3), whereas other related parameters including WC_0, RWC_{TLP}, π_0 and ε_0 showed no significant differences. The g_{min} values were the greatest for upslope trees (table3). Although, there were large differences in needle dimensions (figure 1) according to the tree locations, the H_v were similar between tree groups (table 3).

The risk for xylem hydraulic failure according to the location was evaluated in two ways: i) by calculating the hydraulic safety margin, ii) by simulating the impact of a drought on the dynamics of xylem embolism with the *SurEau* model. We calculated the hydraulic safety margin as the difference between P_{50} and the Ψ_{TLP}. The former is considered as a threshold in

hydraulic failure for conifers, while the latter is a proxy of the water potential inducing stomatal closure delaying embolism occurrence. The figure 4B shows that this safety margin was significantly higher for slope trees (mean of 1.92 MPa) compared to downslope trees (1.18 MPa), upslope trees having an intermediate mean value (1.53 MPa). Using the experimental trait values and the pedo-climatic conditions, the computations of the *SurEau* model revealed that the PLC dynamics showed differences between tree locations (figure 6). Xylem embolism increased later in downslope trees comparing to slope and upslope trees (figure 6A). Finally, there was no difference in xylem embolism dynamic between slope and upslope trees. However, when trees were submitted to similar drought conditions, i.e. drought at downslope or slope position (Figure 6B and C, respectively), hydraulic failure was delayed in trees grown at slope position compared to trees grown on upslope or on downslope.

Discussion

Scots pines settled and developed on the slopes were subject to the most severe stress conditions as they have a dwarf phenotype associated with severe reductions in growth, needle dimensions and chlorophyll content. These slope trees showed the greatest hydraulic safety margin and were operating with the highest water potentials to avoid embolism events. This hydraulic safety seems to be prioritized over growth. These trees also presented reduced photosynthetic properties as they had a reduced hydraulic conductivity, a low quantity of photosynthetic pigments, and bulk leaf parameters such as π_0, Ψ_{TLP}, and ε_0 unfavorable to gas exchange. Scots pines developed under intermediate stress conditions, i.e. on upper slope, showed intermediate hydraulic adjustments.

The physiological and morphological adjustments in Scots pines settled and developed under very stressful conditions were quite different from those observed for the same species between populations located along environmental gradients throughout Europe (Martinez-Vilalta et al. 2009; Rosas et al. 2019). For instance, we observed a decrease in stem conductivity and

vulnerability to embolism, no change in H_v and an increase in SLA for slope trees, whereas populations developed on drier sites at the European scale showed no change in stem hydraulic traits, an increase in *Hv* and a decrease in SLA (Martinez-vilalta et al. 2009; Rosas et al. 2019). This confirms the interest in investigating the tree response over long periods of time and under more constraining conditions, in particular drier and hotter than those encountered in the current range of the species.

Responses of Scots pines to the harsh conditions of slag slopes

All the slope trees are homogeneous in height and age, indicating that they germinated at the same time, probably when conditions allowed seedlings to settle. The observed response of the studied trees could be explained by both a selection process of the most resistant genotype and having a phenotypic plasticity adapted to this environment. In support of this assumption, greatest plasticity induced by water-limited conditions was found for genotypes originated from a warm dry site, with enhanced drought tolerance compared with the genotype from a cool-wet site (Challis et al. 2022).

The weak growth in slope trees, and to a lesser extent in upslope trees (figure 2), resulted in a dwarf phenotype (figure 1). This phenotype would be related to a decrease in parameters related to photosynthetic capacities, such as photosynthetic pigment contents, N content and needle dimensions (table 2 and 3). Since the three conditions are a few meters apart (a dozen at most), the slope factor would mainly affect water availability and nutrient content (Frain 1991). According to the results on the nutrient assays (table 1), Scots pines did not suffer from any deficiency for the nutrient assayed, except for N that was at lower content in both slope and upslope trees. This lower N content was already reported as correlated with a decrease in chlorophyll and carotenoids contents and an increase in the chlorophyll a/b ratio (Mu and Chen 2021). These changes in pigment contents and ratio have also been reported for Scots pines under prolonged drought conditions (Zlobin et al. 2019). This was attributed to a limited

capacity to absorb nitrogen (Salazar-Tortosa et al. 2018; Zlobin et al. 2019). Under prolonged drought conditions, Scots pines would be trapped in a feedback cycle of nutrient deficit that would exacerbate the detrimental impacts of drought on growth (Salazar-Tortosa et al. 2018). It is thus difficult to dissociate nutritional effect from drought effects, especially on long-term responses. The vulnerability to embolism is known to decrease under drier conditions (Awad et al. 2010; Lemaire et al. 2021), but the effect of nitrogen availability on the hydraulic traits are contradictory among studies (e.g. Hacke et al. 2010; Plavcová et al. 2012; Borghetti et al. 2017). It is thus difficult to analyze the cause of the phenotypic responses in our study. However, some parameters such as growth and photosynthetic pigment contents indicated that slope trees were more stressed than upslope trees, while they showed the same nitrogen content. This suggests that the phenotype of slope trees would be more associated with a water deficiency though it was not recorded during our sampling time.

Prioritizing hydraulic safety in slope trees

Slope trees showed lower vulnerability to embolism than the downslope trees. Several studies have shown that vulnerability to embolism decreases when plants grow under drier conditions; this trait being designed according to the water potential experienced by the plant at the time of xylem formation (Awad et al. 2010; Lemaire et al. 2021). Yet, Scots pine populations growing under very dry conditions do not show changes in their vulnerability to embolism, but rather acclimation of other traits such as Hv, K_s and Ψ_{TLP} (Martinez-Vilalta et al. 2009; Rosas et al. 2019). Studies on other species concluded the same lack of relationship between climate dryness and vulnerability to embolism (e.g. Herbette et al. 2010; Wortemman et al. 2011; Hajek et al. 2016). A reduction in the vulnerability to embolism would only be possible for the most marginal populations (Stojnic et al. 2017). This is consistent with the fact that slope pines in this study were in conditions at the limit of their ecological niche. It remains

to determine if this results from acclimation or from selection of individuals having the lowest vulnerability to embolism.

Slope pines had also a higher Ψ_{TLP} compared to downslope trees, limiting water loss through early stomatal closure. This is consistent with a stabilization of Ψ_{md} at higher values during the season and on a dry day for slope trees, compared to other conditions (Figure 3). This appears contradictory to the results from Rosas et al (2019) showing a lower Ψ_{TLP} for Scots pine populations growing on very dry sites. As for vulnerability to embolism, such discrepancy could be related to the fact that the slope pines were in very stressful conditions, and they should ensure their survival rather than an efficient growth. The resulting safety margin is significantly increased in these slope pines. The simulated dynamics of xylem embolism support this improved safety margin for slope trees since the increase in xylem embolism was delayed for slope trees compared to other trees when they were submitted to similar drought conditions (Figure 6B and C). Moreover, the slope trees maintained the lowest g_{min} value, whereas g_{min} was the highest in upslope trees (table 3). This hydraulic safety showed its effectiveness by very low levels of embolism accumulated over the previous years (figure 5). Moreover, the most surprising point is that these trees do not seem to be in a more constrained water status, as revealed by the 2 years of monitoring of water potentials (figure 3). A recent study on grapevine based on model-assisted ideotyping demonstrated that, among the various trait combinations tested, the most drought-tolerant plants had generally a larger hydraulic safety margin (Dayer et al. 2022). In our study, the harsh conditions imposed by the slag slopes favored the development of a large hydraulic safety margin.

This greater hydraulic safety in slope pines would be ensured at the expense of growth, and thus contributes to the dwarf phenotype of the slope pines. First, there is a carbon cost associated with the development of embolism-resistant xylem (Hacke et al. 2001). In a previous study, we demonstrated that a decrease in vulnerability to embolism was prioritized over the

445 growth for beech recovering from a severe drought (Herbette et al. 2021). Accordingly, we
446 observed a higher wood density for slope pines (data not shown), a trait that is usually correlated
447 with vulnerability to embolism and requires an energy cost (Hacke et al. 2001). The earlier
448 closure of stomata deduced from Ψ_{TLP} led to a reduction in carbon assimilation which would
449 further explain the poor growth of slope pines, in addition to reductions in chlorophyll and
450 nitrogen contents and needle size. The needles of these slope pines also showed an increase in
451 π_0 and an increase in ε_0 which could be associated with decreases in soluble sugar content and
452 wall thickness, related to a lower photosynthetic activity in these pines.

453 **Conclusions**

454 Scots pines that had grown for several years under stressful conditions showed
455 physiological adjustments that increased their hydraulic safety at the expense of their growth.
456 Contrary to our initial hypotheses, the slope trees did not operate with a higher hydraulic risk
457 and a sub-lethal embolism threshold, but with a lower hydraulic risk than the upslope and
458 downslope pines having a higher growth rate. On the long term, hydraulic safety is prioritized
459 over growth that just barely allowed for renewal of structures.

460 This study helps to improve our forecasts on the response of Scots pine populations to
461 climate change that will be accompanied by intense and recurrent droughts over several years.
462 Of course, such a study does not integrate the interactions between species in the response to
463 climate change, and in particular the competition by more xerophilic species. The next step of
464 this work will be to distinguish the role of plasticity from that of a selection effect on these
465 physiological adjustments.

466

467 **Supplementary data.**

468 Table S1. Exhaustive list of variables used for *SurEau* simulations.

469 **Conflict of Interest.**

The authors declare that the research was conducted in the absence of any commercial or financial relationships that could be construed as a potential conflict of interest.

Authors' contributions

HC, SH and STB contributed to developing the question and experimental design. DSFF, DMSP, HC, JN, PH, SH and STB performed ecophysiological analyses. ME and SH handled experiments dealing with nutrient, chlorophyll and carotenoid contents. EB and PC conducted microCT experiments. STB, HC and SH wrote the manuscript with contributions from all authors.

References

Allen CD, Macalady AK, Chenchouni H, Bachelet D, McDowell N, Vennetier M, Kitzberger T, Rigling A, Breshears DD, Hogg EH, Gonzalez P, Fensham R, Zhang Z, Castro J, Demidova N, Lim J-H, Allard G, Running SW, Semerci A, Cobb N (2010) A global overview of drought and heat-induced tree mortality reveals emerging climate change risks for forests. Forest Ecology and Management. 259:660-684.

Anderegg WR (2015) Spatial and temporal variation in plant hydraulic traits and their relevance for climate change impacts on vegetation. New Phytol. 205:1008-14.

Anderegg WR, Klein T, Bartlett M, Sack L, Pellegrini AF, Choat B, Jansen S (2016) Meta-analysis reveals that hydraulic traits explain cross-species patterns of drought-induced tree mortality across the globe. Proc Natl Acad Sci U S A. 113:5024-9.

Anderson-Teixeira KJ, Miller AD, Mohan JE, Hudiburg TW, Duval BD, Delucia EH (2013) Altered dynamics of forest recovery under a changing climate. Glob Chang Biol. 19:2001-21.

Awad H, Barigah T, Badel E, Cochard H, Herbette S (2010) Poplar vulnerability to xylem cavitation acclimates to drier soil conditions. Physiol Plant. 139:280-8.

Barbeta A, Ogaya R, Penuelas J (2013) Dampening effects of long-term experimental drought on growth and mortality rates of a Holm oak forest. Glob Chang Biol. 19:3133-44.

Barigah TS, Charrier O, Douris M, Bonhomme M, Herbette S, Ameglio T, Fichot R, Brignolas F, Cochard H (2013) Water stress-induced xylem hydraulic failure is a causal factor of tree mortality in beech and poplar. Ann Bot. 112:1431-7.

Bartlett MK, Scoffoni C, Sack L (2012) The determinants of leaf turgor loss point and prediction of drought tolerance of species and biomes: a global meta-analysis. Ecol Lett. 15:393-405.

Bartlett MK, Zhang Y, Kreidler N, Sun S, Ardy R, Cao K, Sack L (2014) Global analysis of plasticity in turgor loss point, a key drought tolerance trait. Ecology Letters. 17:1580-1590.

Berg MP, Ellers J (2010) Trait plasticity in species interactions: a driving force of community dynamics. Evolutionary Ecology. 24:617-629.

Borghetti M, Gentilesca T, Leonardi S, van Noije T, Rita A, Mencuccini M (2017) Long-term temporal relationships between environmental conditions and xylem functional traits: a meta-analysis across a range of woody species along climatic and nitrogen deposition gradients. Tree Physiol. 37:4-17.

Brodribb TJ, McAdam SA, Jordan GJ, Martins SC (2014) Conifer species adapt to low-rainfall climates by following one of two divergent pathways. Proc Natl Acad Sci U S A. 111:14489-93.

Brodribb TJ, Powers J, Cochard H, Choat B (2020) Hanging by a thread? Forests and drought. Science. 368:261-266.

Challis A, Blackman C, Ahrens C, Medlyn B, Rymer P, Tissue D (2022) Adaptive plasticity in plant traits increases time to hydraulic failure under drought in a foundation tree. Tree Physiol. 42:708-721.

520 Chaves MM, Maroco JP, Pereira JS (2003) Understanding plant responses to drought - from
521 genes to the whole plant. Functional Plant Biology. 30:239-264.
522 Choat B, Jansen S, Brodribb TJ, Cochard H, Delzon S, Bhaskar R, Bucci SJ, Feild TS, Gleason
523 SM, Hacke UG, Jacobsen AL, Lens F, Maherali H, Martinez-Vilalta J, Mayr S,
524 Mencuccini M, Mitchell PJ, Nardini A, Pittermann J, Pratt RB, Sperry JS, Westoby M,
525 Wright IJ, Zanne AE (2012) Global convergence in the vulnerability of forests to
526 drought. Nature. 491:752-756.
527 Cochard H (2021) A new mechanism for tree mortality due to drought and heatwaves. Peer
528 Community Journal. 1, e36.
529 Cochard H, Damour G, Bodet C, Tharwat I, Poirier M, Ameglio T (2005) Evaluation of a new
530 centrifuge technique for rapid generation of xylem vulnerability curves. Physiologia
531 Plantarum. 124:410-418.
532 Cochard H, Delzon S, Badel E (2015) X-ray microtomography (micro-CT): a reference
533 technology for high-resolution quantification of xylem embolism in trees. Plant Cell
534 Environ. 38:201-6.
535 Cotrufo MF, Alberti G, Inglima I, Marjanović H, LeCain D, Zaldei A, Peressotti A, Miglietta
536 F (2011) Decreased summer drought affects plant productivity and soil carbon dynamics
537 in a Mediterranean woodland. Biogeosciences. 8:2729-2739.
538 Dayer S, Lamarque LJ, Burlett R, Bortolami G, Delzon S, Herrera JC, Cochard H, Gambetta
539 GA (2022) Model-assisted ideotyping reveals trait syndromes to adapt viticulture to a
540 drier climate. Plant Physiology
541 Duursma RA, Blackman CJ, Lopez R, Martin-StPaul NK, Cochard H, Medlyn BE (2019) On
542 the minimum leaf conductance: its role in models of plant water use, and ecological and
543 environmental controls. New Phytol. 221:693-705.
544 Feichtinger LM, Eilmann B, Buchmann N, Rigling A (2014) Growth adjustments of conifers

545 to drought and to century-long irrigation. Forest Ecology and Management. 334:96-105.
546 Feichtinger LM, Eilmann B, Buchmann N, Rigling A (2015) Trait-specific responses of Scots
547 pine to irrigation on a short vs long time scale. Tree Physiol. 35:160-71.
548 Fernández-de-Uña L, Aranda I, Rossi S, Fonti P, Cañellas I, Gea-Izquierdo G (2018) Divergent
549 phenological and leaf gas exchange strategies of two competing tree species drive
550 contrasting responses to drought at their altitudinal boundary. Tree Physiology.
551 38:1152-1165.
552 Frain M. 1991. Approche phytosociologique de la dynamique des végétations primaires sur
553 roches artificiellement denudées en Auvergne, Velay et Limousin. Clermont-Ferrand 2.
554 Goldstein G, Bucci SJ, Scholz FG (2013) Why do trees adjust water relations and hydraulic
555 architecture in response to nutrient availability? Tree Physiol. 33:238-40.
556 González-Muñoz N, Sterck F, Torres-Ruiz JM, Petit G, Cochard H, von Arx G, Lintunen A,
557 Caldeira MC, Capdeville G, Copini P, Gebauer R, Grönlund L, Hölttä T, Lobo-do-Vale
558 R, Peltoniemi M, Stritih A, Urban J, Delzon S (2018) Quantifying in situ phenotypic
559 variability in the hydraulic properties of four tree species across their distribution range
560 in Europe. PLoS One. 13
561 Hacke UG, Plavcová L, Almeida-Rodriguez A, King-Jones S, Zhou W, Cooke JEK (2010)
562 Influence of nitrogen fertilization on xylem traits and aquaporin expression in stems of
563 hybrid poplar. Tree Physiology. 30:1016-1025.
564 Hacke UG, Sperry JS, Pockman WT, Davis SD, McCulloh KA (2001) Trends in wood density
565 and structure are linked to prevention of xylem implosion by negative pressure.
566 Oecologia. 126:457-461.
567 Hajek P, Kurjak D, von Wühlisch G, Delzon S, Schuldt B (2016) Intraspecific variation in wood
568 anatomical, hydraulic, and foliar traits in ten European beech provenances differing in
569 growth yield. Frontiers in plant science. 7:791.

570 Herbette S, Charrier O, Cochard H, Barigah TS (2021) Delayed effect of drought on xylem
571 vulnerability to embolism in Fagus sylvatica. Canadian Journal of Forest Research.
572 51:622-626.
573 Herbette S, Wortemann R, Awad H, Huc R, Cochard H, Barigah TS (2010) Insights into xylem
574 vulnerability to cavitation in Fagus sylvatica L.: phenotypic and environmental sources
575 of variability. Tree Physiol. 30:1448-55.
576 Jacobsen AL, Pratt RB, Davis SD, Ewers FW (2007) Cavitation resistance and seasonal
577 hydraulics differ among three arid Californian plant communities. Plant Cell Environ.
578 30:1599-609.
579 Kjeldahl J (1183) Neue Methods zur Bestimmung des Stickstoffs in Organischen Korpern. Z
580 Anal Chem. 22:366–382.
581 Lamy JB, Bouffier L, Burlett R, Plomion C, Cochard H, Delzon S (2011) Uniform selection as
582 a primary force reducing population genetic differentiation of cavitation resistance
583 across a species range. PLoS One. 6:e23476.
584 Lemaire C, Blackman CJ, Cochard H, Menezes-Silva PE, Torres-Ruiz JM, Herbette S (2021)
585 Acclimation of hydraulic and morphological traits to water deficit delays hydraulic
586 failure during simulated drought in poplar. Tree Physiol. 41:2008-2021.
587 Leuzinger S, Luo Y, Beier C, Dieleman W, Vicca S, Korner C (2011) Do global change
588 experiments overestimate impacts on terrestrial ecosystems? Trends Ecol Evol. 26:236-
589 41.
590 Lloret F, Peñuelas J, Prieto P, Llorens L, Estiarte M (2009) Plant community changes induced
591 by experimental climate change: Seedling and adult species composition. Perspectives
592 in Plant Ecology, Evolution and Systematics. 11:53-63.
593 Lopez R, Lopez de Heredia U, Collada C, Cano FJ, Emerson BC, Cochard H, Gil L (2013)
594 Vulnerability to cavitation, hydraulic efficiency, growth and survival in an insular pine

595 (Pinus canariensis). Ann Bot. 111:1167-79.
596 MacKay SL, Arain MA, Khomik M, Brodeur JJ, Schumacher J, Hartmann H, Peichl M (2012)
597 The impact of induced drought on transpiration and growth in a temperate pine
598 plantation forest. Hydrological Processes. 26:1779-1791.
599 Maherali H, Pockman WT, Jackson RB (2004) Adaptive variation in the vulnerability of woody
600 plants to xylem cavitation. Ecology. 85:2184-2199.
601 Mantova M, Herbette S, Cochard H, Torres-Ruiz JM (2022) Hydraulic failure and tree
602 mortality: from correlation to causation. Trends Plant Sci. 27:335-345.
603 Martinez-Vilalta J, Cochard H, Mencuccini M, Sterck F, Herrero A, Korhonen JFJ, Llorens P,
604 Nikinmaa E, Nole A, Poyatos R, Ripullone F, Sass-Klaassen U, Zweifel R (2009)
605 Hydraulic adjustment of Scots pine across Europe. New Phytologist. 184:353-364.
606 Martínez-Vilalta J, Prat E, Oliveras I, Piñol J (2002) Xylem hydraulic properties of roots and
607 stems of nine Mediterranean woody species. Oecologia. 133:19-29.
608 Martinez-Vilalta J, Sala A, Piñol J (2004) The hydraulic architecture of Pinaceae - a review.
609 Plant Ecology. 171:3-13.
610 Martin-StPaul N, Delzon S, Cochard H (2017) Plant resistance to drought depends on timely
611 stomatal closure. Ecol Lett. 20:1437-1447.
612 McDowell NG (2011) Mechanisms linking drought, hydraulics, carbon metabolism, and
613 vegetation mortality. Plant Physiol. 155:1051-9.
614 Mencuccini M, Bonosi L (2001) Leaf/sapwood area ratios in Scots pine show acclimation
615 across Europe. Canadian Journal of Forest Research. 31:442-456.
616 Minocha R, Martinez G, Lyons B, Long S (2009) Development of a standardized methodology
617 for quantifying total chlorophyll and carotenoids from foliage of hardwood and conifer
618 tree species. Canadian Journal of Forest Research. 39:849-861.
619 Moreno M, Simioni G, Cailleret M, Ruffault J, Badel E, Carrière S, Davi H, Gavinet J, Huc R,

Limousin JM, Marloie O, Martin L, Rodriguez-Calcerrada JS, Vennetier M, Martin-StPaul NK (2021) Consistently lower sap velocity and growth over nine years of rainfall exclusion in a Mediterranean mixed pine-oak forest. Agricultural and Forest Meteorology. 308-309:108472.

Mu X, Chen Y (2021) The physiological response of photosynthesis to nitrogen deficiency. Plant Physiol Biochem. 158:76-82.

Nicotra AB, Atkin OK, Bonser SP, Davidson AM, Finnegan EJ, Mathesius U, Poot P, Purugganan MD, Richards CL, Valladares F, van Kleunen M (2010) Plant phenotypic plasticity in a changing climate. Trends Plant Sci. 15:684-92.

Pammenter NW, Willigen CV (1998) A mathematical and statistical analysis of the curves illustrating vulnerability of xylem to cavitation. Tree Physiology. 18:589-593.

Paula BN, Chandaa S, Dasa S, Singha P, Pandeya BK, Girib SS (2014) Mineral Assay in Atomic Absorption Spectroscopy. The Beats Nat Sci. 4 (1):1-17.

Plavcová L, Hacke UG (2012) Phenotypic and developmental plasticity of xylem in hybrid poplar saplings subjected to experimental drought, nitrogen fertilization, and shading. Journal of Experimental Botany. 63:6481-6491.

Poyatos R, Martinez-Vilalta J, Cermak J, Ceulemans R, Granier A, Irvine J, Kostner B, Lagergren F, Meiresonne L, Nadezhdina N, Zimmermann R, Llorens P, Mencuccini M (2007) Plasticity in hydraulic architecture of Scots pine across Eurasia. Oecologia. 153:245-59.

Pritzkow C, Williamson V, Szota C, Trouve R, Arndt SK (2020) Phenotypic plasticity and genetic adaptation of functional traits influences intra-specific variation in hydraulic efficiency and safety. Tree Physiol. 40:215-229.

Richardson DM, Rundel PW (1998) Ecology and biogeography of *Pinus*: An introduction. In: Richardson DM (ed) Ecology and Biogeography of *Pinus*. Cambridge University Press,

645 Cambridge, UK, pp 3-46.
646 Rosas T, Mencuccini M, Barba J, Cochard H, Saura-Mas S, Martínez-Vilalta J (2019)
647 Adjustments and coordination of hydraulic, leaf and stem traits along a water
648 availability gradient. New Phytologist. 223:632-646.
649 Sack L, Pasquet-Kok J. 2010. Leaf pressure-volume curve parameters. PrometheusWiki.
650 Salazar-Tortosa D, Castro J, Villar-Salvador P, Vinegla B, Matias L, Michelsen A, Rubio de
651 Casas R, Querejeta JI (2018) The "isohydric trap": A proposed feedback between water
652 shortage, stomatal regulation, and nutrient acquisition drives differential growth and
653 survival of European pines under climatic dryness. Glob Chang Biol. 24:4069-4083.
654 Seidel H, Menzel A (2016) Above-Ground Dimensions and Acclimation Explain Variation in
655 Drought Mortality of Scots Pine Seedlings from Various Provenances. Front Plant Sci.
656 7:1014.
657 Stojnić S, Suchocka M, Benito-Garzón M, Torres-Ruiz JM, Cochard H, Bolte A, Cocozza C,
658 Cvjetković B, de Luis M, Martinez-Vilalta J, Ræbild A, Tognetti R, Delzon S (2017)
659 Variation in xylem vulnerability to embolism in European beech from geographically
660 marginal populations. Tree Physiology. 38:173-185.
661 Sultan SE (2000) Phenotypic plasticity for plant development, function and life history. Trends
662 Plant Sci. 5:537-42.
663 Tyree MT, Hammel HT (1972) The measurement of the turgor pressure and the water relations
664 of plants by the pressure-bomb technique. Journal of Experimental Botany. 23:267-282.
665 Wortemann R, Herbette S, Barigah TS, Fumanal B, Alia R, Ducousso A, Gomory D, Roeckel-
666 Drevet P, Cochard H (2011) Genotypic variability and phenotypic plasticity of
667 cavitation resistance in Fagus sylvatica L. across Europe. Tree Physiol. 31:1175-82.
668 Wright IJ, Reich PB, Westoby M, Ackerly DD, Baruch Z, Bongers F, Cavender-Bares J, Chapin
669 T, Cornelissen JH, Diemer M, Flexas J, Garnier E, Groom PK, Gulias J, Hikosaka K,

Lamont BB, Lee T, Lee W, Lusk C, Midgley JJ, Navas ML, Niinemets U, Oleksyn J, Osada N, Poorter H, Poot P, Prior L, Pyankov VI, Roumet C, Thomas SC, Tjoelker MG, Veneklaas EJ, Villar R (2004) The worldwide leaf economics spectrum. Nature. 428:821-7.

Zang C, Pretzsch H, Rothe A (2012) Size-dependent responses to summer drought in Scots pine, Norway spruce and common oak. Trees. 26:557-569.

Zlobin IE, Kartashov AV, Pashkovskiy PP, Ivanov YV, Kreslavski VD, Kuznetsov VV (2019) Comparative photosynthetic responses of Norway spruce and Scots pine seedlings to prolonged water deficiency. J Photochem Photobiol B. 201:111659.

List of figures

Figure 1: Study site and morphology of the studied trees. The study site is located on a former quarry of the volcano "Puy de la Vache". The site is organized in terraces of slag separated by slopes. The vegetation present on these slopes and terraces has developed without any human intervention. On the slopes, the only vascular species to develop is the Scots pine. The site is split into 3 areas: the slope, the upslope (corresponding to a terrace) and the downslope (corresponding to the bottom of the quarry). The box shows the morphology of branches developed by slope, upslope and downslope trees, from left to right, respectively.

Figure 2: Annual ring growth of branch samples from Scots pines developed under the three conditions. Branches were sampled on trees located on the downslope (square), the upslope (circle) or the slope (cross). Their annual ring growth were measured and plotted versus their age. Each point represents one branch from one individual tree. Points showing error bars (± SD) are mean values, and different uppercase and lowercase letters indicate significant differences between conditions for annual ring growth and sample age, respectively ($P < 0.05$).

Figure 3: Seasonal variations (A) and daily time course (B) in xylem water potential of Scots pines developed under the three conditions. A, Midday water potentials were measured on tips of branches sampled from five trees located on the downslope (white), the upslope (grey) or the slope (dark), during sunny days preceded by a period of several days without rain. B, Water potentials were measured regularly from predawn (4 am) to the end (5 pm) of the day 233 on branches sampled from 5 trees located on the downslope (square), the upslope (circle) or the slope (cross). Symbols are mean values, bars represent standard errors, and different letters indicate significant differences between the conditions for each time ($P < 0.05$).

Figure 4: Xylem vulnerability to embolism (A) and hydraulic safety margin (B) of branches from Scots pines developed under the three conditions. A, vulnerability curves were performed from measurements on branches sampled from 6 trees located on the

downslope (solid line), on the upslope (dashed line) or on the slope (dotted line). For each curve, the mean water potential at 50% loss of hydraulic conductance (P_{50}) is indicated by the open symbol and the error bar is the standard error. B, the hydraulic safety margin was calculated for each tree from the difference between and Ψ_{TLP} and P_{50} values. Mean values and standard errors are represented. Different letters indicate significant differences between the conditions ($P < 0.01$).

Figure 5: Transverse X-ray microtomography images of branches from Scots pines developed under the three conditions. Branches were sampled from trees developed at the downslope (A, D), at the upslope (B, E) or at the slope (C, F). Embolized tracheids are as depicted by black color while the fully saturated tissues are depicted as bright color. Embolized conduits were mainly found for the oldest wood rings. No embolism (or few) was observed in the rings of the last two years.

Figure 6: Simulated (*SurEau* model) time courses of the loss of xylem hydraulic conductance in the branches during a virtual drought event. Drought simulations were performed using experimental traits values from trees developing on the downslope (solid lines), on the upslope (dashed lines) or on the slope (dotted lines), while considering three conditions: trees in their respective locations (A), all trees on the downslope (B) and all trees on the slope (C)**.**

724

Element content (mg.g^{-1} DW)	Downslope	Upslope	Slope
Nitrogen	12.85(± 1.03)[a]	8.54 (± 0.35)[b]	7.16 (± 0.49)[b]
Potassium	7.64 (± 0.55)	6.89 (± 0.29)	7.50 (± 0.38)
Calcium	14.3 (± 0.79)	13.4 (± 0.76)	14.7 (± 0.39)
Magnesium	4.65 (± 0.22)	4.87 (± 0.12)	5.49 (± 0.33)
Iron	0.451 (± 0.027)	0.514 (± 0.062)	0.494 (± 0.042)
Copper	0.0492 (± 0.0026)	0.0415 (± 0.0054)	0.0416 (± 0.0033)
Zinc	0.0552 (± 0.0021)	0.0450 (± 0.0058)	0.0407 (± 0.0030)

725

726 **Table 1: Nutrient content in needle from Scots pines developed under the three conditions**. Data are mean
727 values (± SE) from three branches per tree sampled from three to five trees developed on the downslope, the
728 upslope and the slope, respectively. Different letters indicate significant differences between the conditions for
729 each element ($P < 0.05$).

Pigment content	Downslope	Upslope	Slope
Total chlorophyll (mg.g^{-1} FW)	1.98 (± 0.20)^{a}	0.99 (± 0.08)^{b}	0.58 (± 0.04)^{c}
Chlorophyll a/b ratio	2.18 (± 0.09)^{a}	2.28(± 0.06)^{a}	2.55(± 0.03)^{b}
Total carotenoids (mg.g^{-1} FW)	0.511 (± 0.049)^{a}	0.261 (± 0.021)^{b}	0.190 (± 0.010)^{c}

730

731 **Table 2: Photosynthetic pigment content in needle from Scots pines developed under the three conditions**.
732 Data are means values (± SE) from 11, 8 and 15 individual trees developed on the downslope, the upslope and the
733 slope, respectively. Different letters indicate significant differences between the conditions for each pigment
734 content ($P < 0.01$).

Traits (units)	Downslope	Upslope	Slope
$P_{50\ stem}$ (MPa)	-3.25 (± 0.05) [a]	-3.49 (± 0.11) [ab]	-3.70 (± 0.07) [b]
*K*s (mol m^{-1} s^{-1} MPa^{-1})	23.3 (± 2.41) [a]	24.4 (± 2.11) [a]	11.5 (± 1.06) [b]
LSC (mmol m^{-1} s^{-1} MPa^{-1})	5.29 (± 0.38)[a]	5.96 (± 0.49) [a]	3.14 ((± 0.41) [b]
SLA (m^2 g^{-1})	80.79 (± 1.14)[a]	67.75 (± 1.48)[b]	108.94 (± 10.24)[c]
H_v ($cm^2.m^{-2}$)	2.62 (± 0.18)	2.70 (± 0.14)	2.64 (± 0.11)
g_{min} (mol m^{-2} s^{-1})	1.91 (± 0.23) [a]	2.79 (± 0.17) [b]	1.64 (± 0.19) [a]
Ψ_{TLP} (MPa)	-2.07 (± 0.11) [a]	-1.87 (± 0.15) [ab]	-1.78 (± 0.10) [b]
WC_0	2.04 (± 0.44)	1.67 (± 0.30)	1.57 (± 0.24)
RWC_{TLP}	70.76 (± 5.91)	75.21(± 4.18)	76.14 (± 3.84)
π_0 (MPa)	-1.36 (± 0.10)	-1.32 (± 0.11)	-1.21 (± 0.08)
ε_0 (MPa)	6.28 (± 1.65)	5.68 (± 1.12)	5.11 (± 1.01)

Table 3: Functional traits for Scots pines developed under the three conditions. Data are the mean values (± SE) and different letters indicate significant difference between the conditions for each trait ($P < 0.05$). ε_0, bulk modulus of tissue elasticity; g_{min}, minimal needle conductance; H_v, Huber value ; *K*s, specific hydraulic conductivity of the branch ; *LSC*, leaf specific conductivity of the branch; P_{50}, pressure inducing 50 % loss of hydraulic conductance; Ψ_{TLP}, water potential at turgor loss point; π_0, osmotic potential at full turgor; RWC_{TLP}, relative water content at turgor loss point *SLA*, specific leaf area ; WC_0, water content at full turgor.

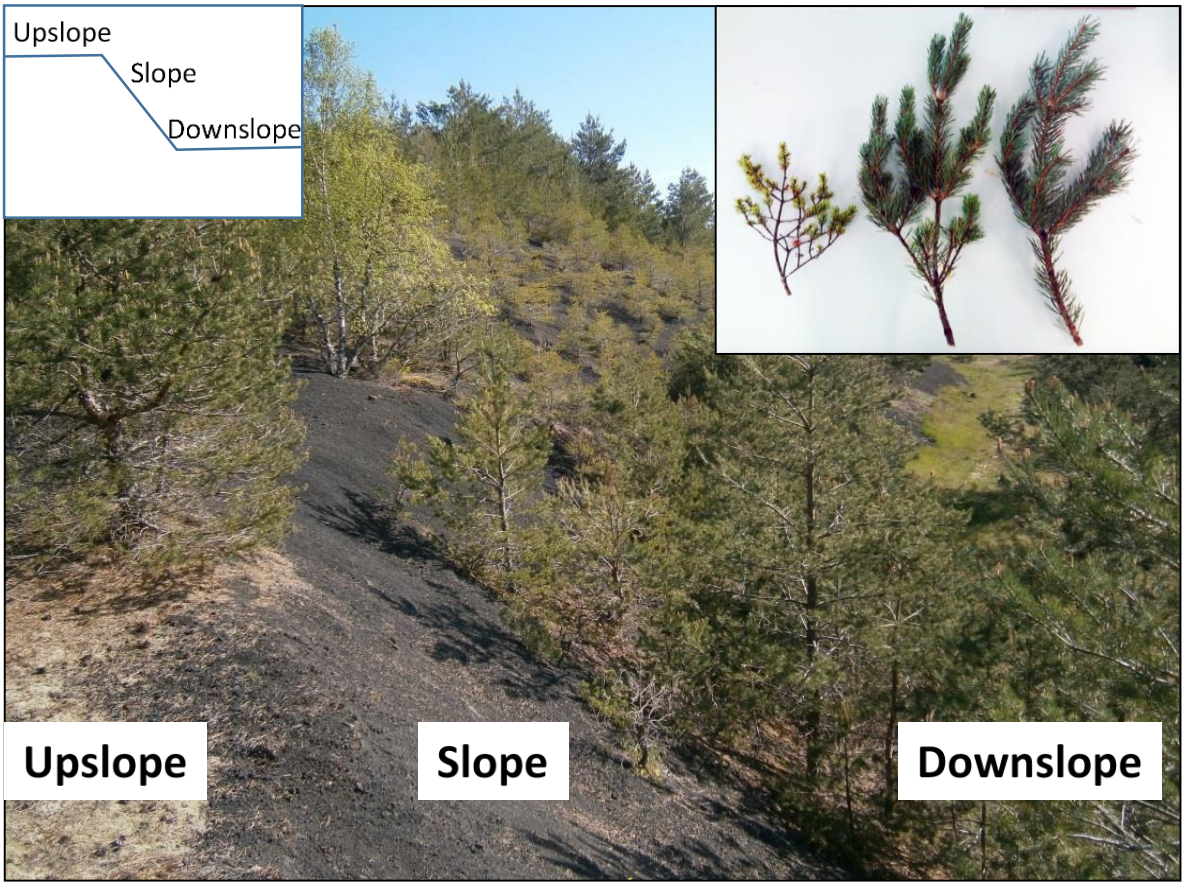

Figure 1: Study site and morphology of the studied trees. The study site is located on a former quarry of the volcano "Puy de la Vache". The site is organized in terraces of slag separated by slopes. The vegetation present on these slopes and terraces has developed without any human intervention. On the slopes, the only vascular species that develops is the Scots pine. The site is split into 3 areas: the slope, the upslope (corresponding to a terrace) and the downslope (corresponding to the bottom of the quarry). The box shows the morphology of branches developed by slope, upslope and downslope trees, from left to right, respectively. We also used this morphological differences to clearly distinguish between the three conditions.

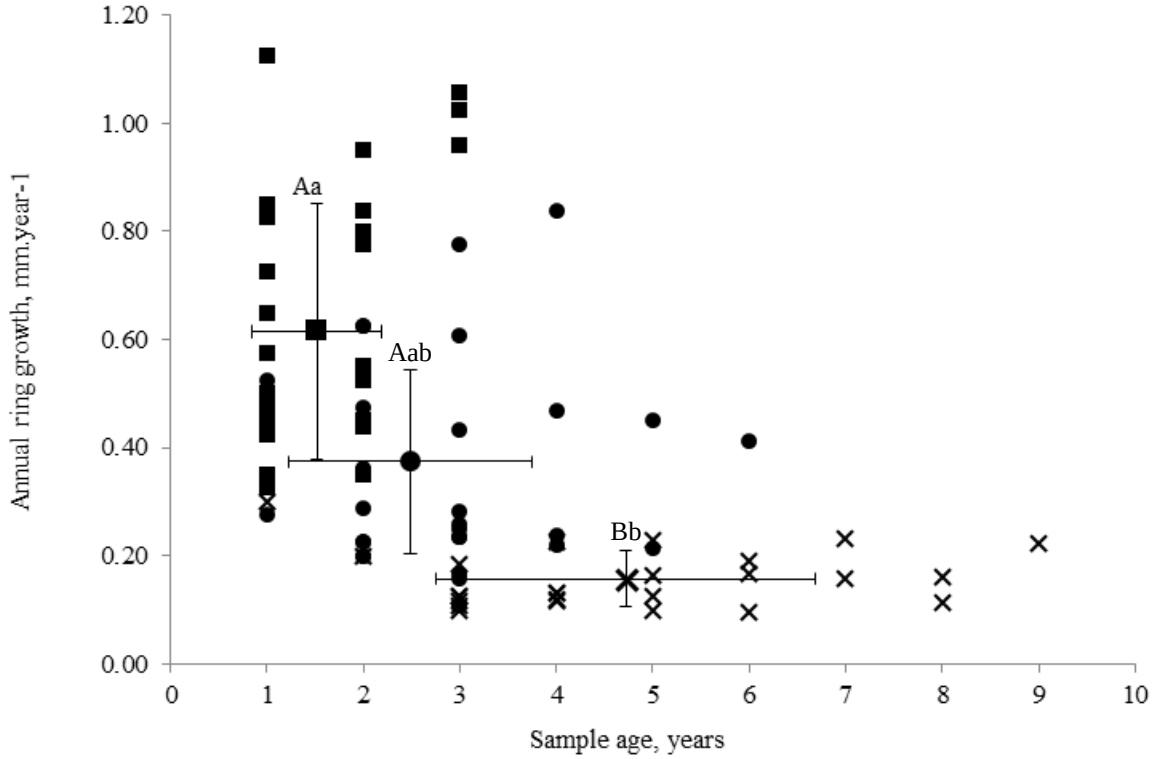

Figure 2: Annual ring growth of branch samples from Scots pines developed under the three conditions. Branches were sampled on trees located on the downslope (square), the upslope (circle) or the slope (cross). Their annual ring growth were measured and plotted versus their age. Each point represents one branch from one individual tree. Points showing error bars (± SD) are mean values, and different uppercase and lowercase letters indicate significant differences between conditions for annual ring growth and sample age, respectively ($P < 0.05$).

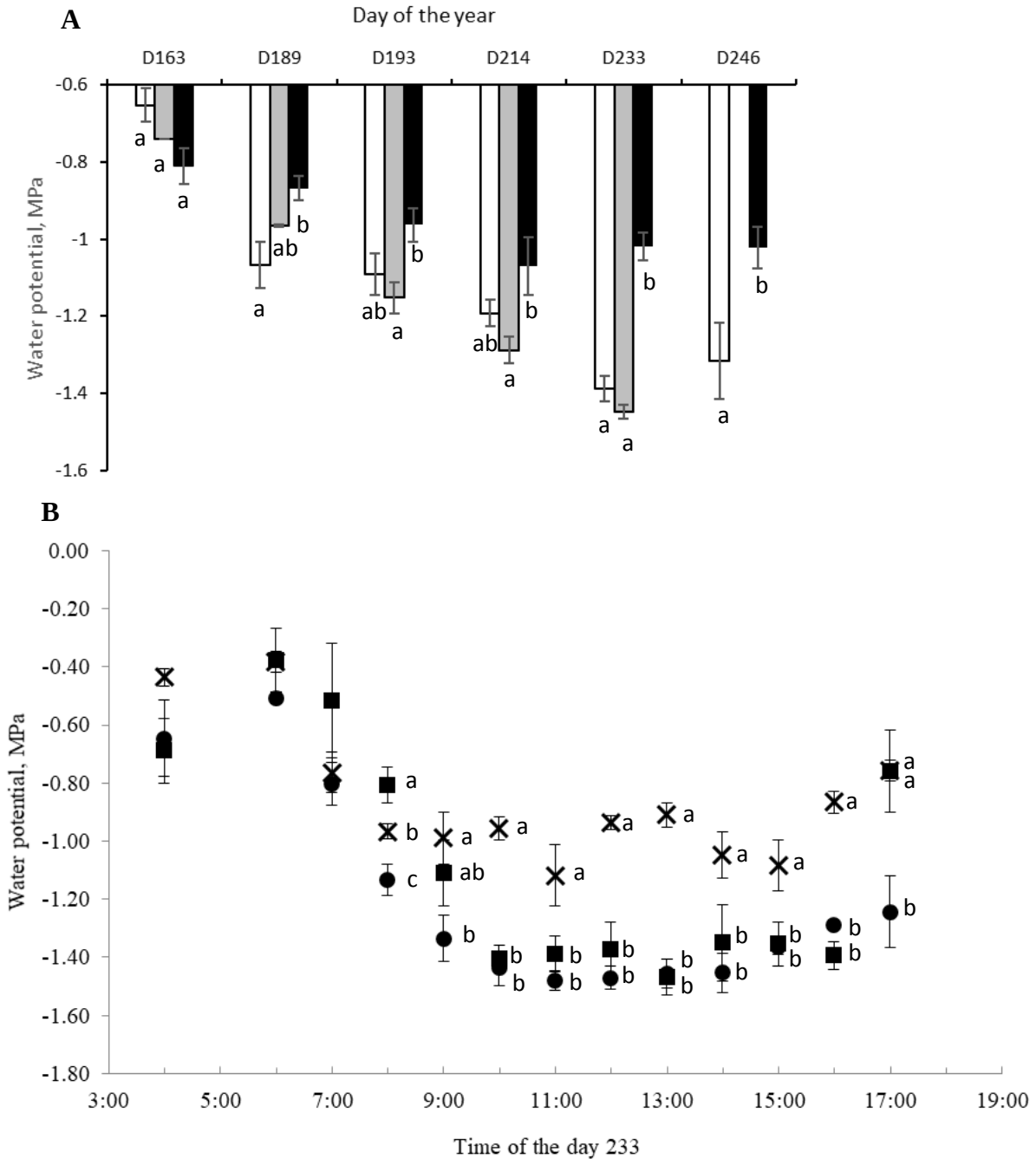

Figure 3: Seasonal variations (A) and daily time course (B) of xylem water potential of Scots pines developed under the three conditions. A, Midday water potentials were measured on tips of branches sampled from five trees located on the downslope (white), the upslope (grey) or the slope (dark), during sunny days preceded by a period of several days without rain. B, Water potentials were measured regularly from predawn (4 am) to the end (5 pm) of the day 233 on branches sampled from 5 trees located on the downslope (square), the upslope (circle) or the slope (cross). Symbols are mean values, bars represent standard errors, and different letters indicate significant differences between the conditions for each time ($P < 0.05$).

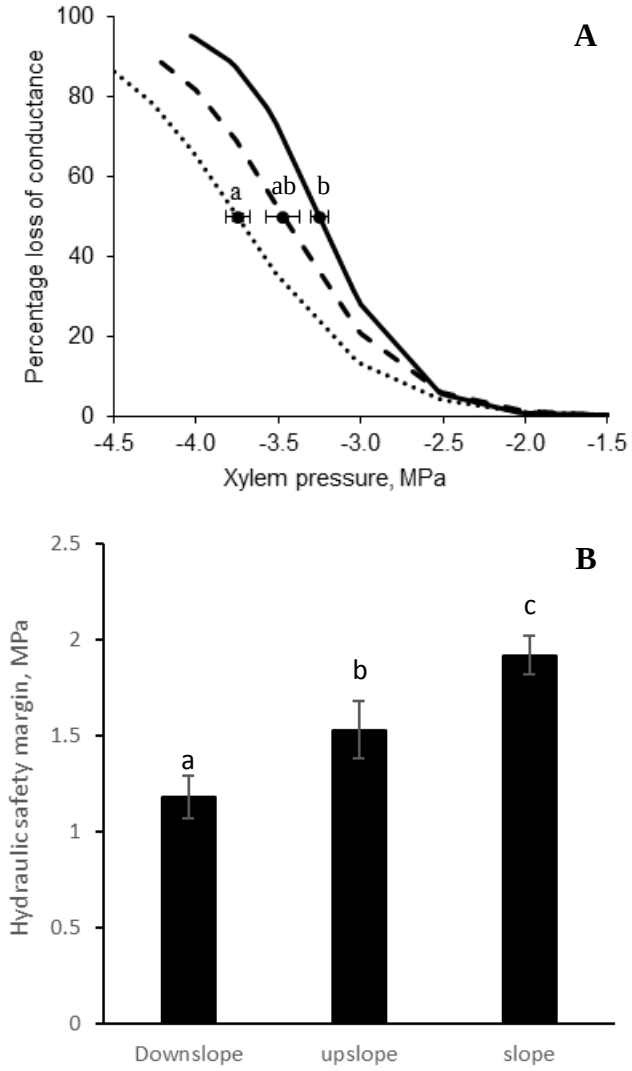

Figure 4: Xylem vulnerability to embolism (A) and hydraulic safety margin (B) of branches from Scots pines developed under the three conditions. A, vulnerability curves were performed from measurements on branches sampled from 6 trees located on the downslope (solid line), on the upslope (dashed line) or on the slope (dotted line). For each curve, the mean water potential at 50% loss of hydraulic conductance (P_{50}) is indicated by the open symbol and the error bar is the standard error. B, the hydraulic safety margin was calculated for each tree from the difference between and Ψ_{TLP} and P_{50} values. Mean values and standard errors are represented. Different letters indicate significant differences between the conditions ($P < 0.01$).

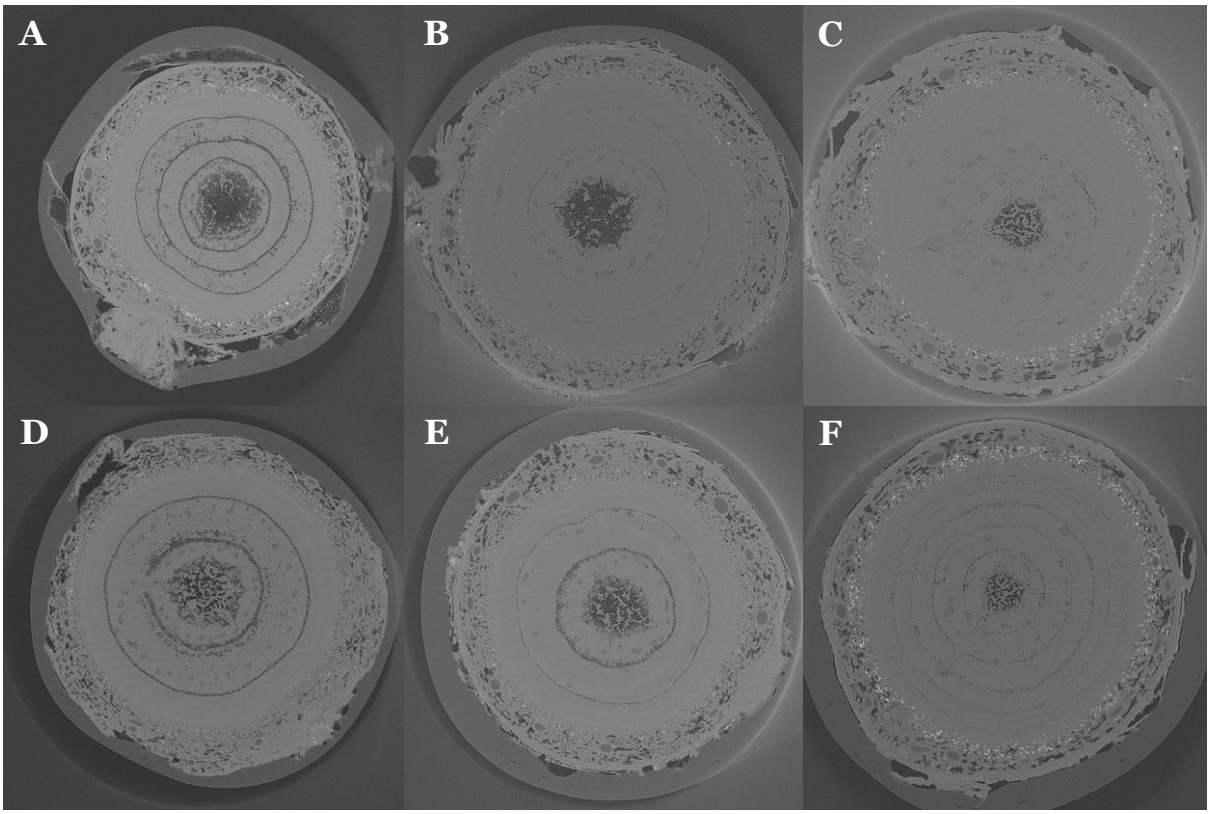

Figure 5: Transverse X-ray microtomography images of branches from Scots pines developed under the three conditions. Branches were sampled from trees developed at the downslope (A, D), at the upslope (B, E) or at the slope (C, F). Embolized tracheids are seen in black while the fully saturated tissues are seen in bright color. Embolized conduits were mainly found for the oldest wood rings. No embolism (or few) was observed in the rings of the last two years.

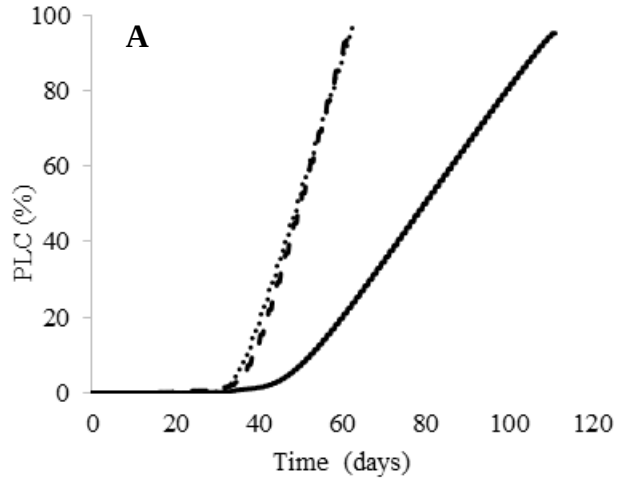

786

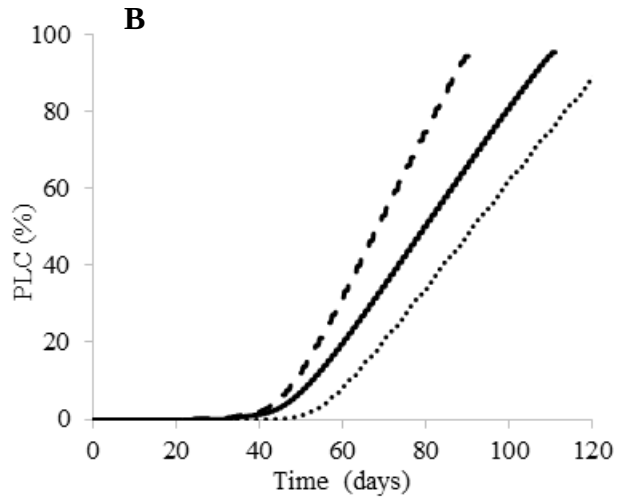

787

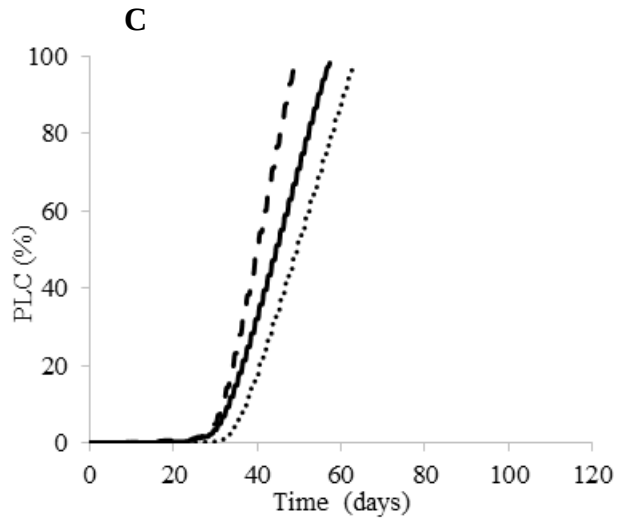

788

789 **Figure 6: Simulated (*SurEau* model) time courses of the loss of xylem hydraulic conductance in the branches**
790 **during a virtual drought event.** Drought simulations were performed using experimental traits values from trees
791 developing on the downslope (solid lines), on the upslope (dashed lines) or on the slope (dotted lines), while
792 considering three conditions: trees in their respective locations (A), all trees on the downslope (B) and all trees on
793 the slope (C)**.**